DTUWEC: an open-source DTU Wind Energy Controller with advanced industrial features

DTUWEC: an open-source DTU Wind Energy Controller with advanced industrial features

Fanzhong Meng, Wai Hou Lio and Thanasis Barlas
Department of Wind Energy, Technical University of Denmark, DK-4000 Roskilde, Denmark
E-mail: famen@dtu.dk

Abstract. An open-source wind turbine controller, DTU Wind Energy Controller (DTUWEC), developed by Technical University of Denmark (DTU), is presented. The DTUWEC includes many advanced features and it is publicly available to the wind energy community. It is envisioned that this research work converts the old version of Basic DTU Wind Energy Controller into a generic, powerful and robust open-source wind turbine controller with a large number of developers and users in both research institutions and industries. DTUWEC is implemented in Fortran and offers the DNV-GL Bladed/OpenFAST style interface. Because of its open-source and modular characters, researchers are able to couple DTUWEC with different aero-elastic simulation codes to investigate the effect of different controllers on the wind turbine structural loads and power output, and to collaborate for future potential improvements.

1. Introduction

The development and improvement of wind turbine aero-servo-elastic simulation software have been one of the main activities within wind turbine research institutes, manufacturers and consulting companies for the last thirty years. A wind turbine is a multi-disciplinary system. Modularizing the wind turbine simulation software becomes increasingly crucial for (i) motivating module sharing across the wind turbine community; (ii) simplifying the procedure for code verification; (iii) improving model performance and (iv) enhancing the flexibility and expandability to enable cross developments of functionalities among the wind energy community. Of the many modules within wind turbine simulation software, the wind turbine controller is one of the most essential modules in terms of code comparison and verification between different research projects and research organizations.

Within the last decade, Department of Wind Energy at the Technical University of Denmark (DTU Wind Energy) has been striving for developing the next generation of wind turbine controllers. The research achievements resulted in the first version of the Basic DTU Wind Energy Controller developed by Hansen and Henriksen [1], which was released as an open-source controller built for high fidelity in-house aero-elastic simulation software HAWC2 [2] in 2013. In addition to the basic functionalities, this version of the controller included a reliable and smooth switch between partial and full load region, drive train damping and tower top fore-aft vibration damping. Later, several advanced control features such as Individual Pitch Controller (IPC) [3], Individual Flap Controller (IFC) [4] and integrated flap controller [5, 6] were implemented as individual modules of the Basic DTU Wind Energy Controller for many externally funded research projects. Besides this, the features required by the industry such

as start-up, emergency stop, rotor speed exclusion, pitch actuator stuck and grid loss, were implemented in order to simulate the full IEC load cases [7].

Meanwhile, there are a number of open-source wind turbine controllers existed in the wind energy community. For example, National Renewable Energy Laboratory (NREL) developed an open-source controller for its NREL 5MW reference turbine model [8]. Similarly, the Delft Center for Systems and Control (DCSC) at Delft University of Technology (TU Delft) provided an open-source baseline wind turbine controller called Delft Research Controller (DRC) [9] to the wind turbine community in 2018, which allows scientists to collaborate and contribute in making continuous improvements.

Given that the Basic DTU Wind Energy Controller is tightly integrated with HAWC2, which is a commercial software, the controller was not widely aware by the rest of the wind energy community. Therefore, in recent years, DTU Wind Energy started to revisit the Basic DTU Wind Energy Controller. DTU Wind Energy Controller (DTUWEC) was then proposed and the objective is to develop an open-source and modular controller with advance features including the key industrial supervisory functions that are lacking in some open-source controllers. The aim of this paper is to provide a comprehensive overview and description of the DTUWEC and its latest development. A generic interface was built to allow other wind turbine aero-elastic simulation codes, such as OpenFAST [10] and DNV-GL Bladed. Furthermore, more advanced features, such as rotor-effective wind speed estimator [11] and de-rating control strategies [12], were developed and implemented in the DTUWEC for wind farm control applications in order to increase total Annual Energy Production (AEP) and reduce structural loads.

2. Controller overview

The DTU Wind Energy Controller presented in this work is a further development of the old version of the Basic DTU Wind Energy controller [1] with newly developed advanced control features and generic interface. A top-level architecture of DTUWEC is shown in Figure 1. The DTU Wind Energy controller is implemented as Dynamic Linked Libraries (DLLs) and coupled with the aero-elastic simulation tools via the `Interface_Gate` function, which initializes the control parameters through an external input file depends on the simulation tool. During the run-time, the control reference signals are computed once per time step via the `update_regulation` function and the control servo actions are returned to the simulation tool through the `control_action` function once per step. At the end of the simulation, the aero-elastic simulation tool closes the control DLLs and ends the simulation.

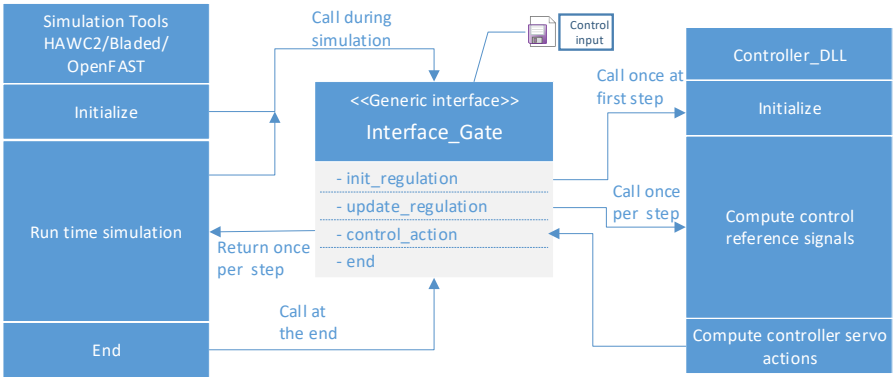

Figure 1: A block diagram of the top-level DTUWEC architecture

The block diagram that describes the functionalities implemented in the DTUWEC is shown in Figure 2. The main controller is responsible for communicating with a simulation tool through

the controller interface. It contains basic control features such as collective pitch, generator torque proportional-integral-derivative (PID) controller and supervisory control features (cut-in, cut-out, emergency stop and system status monitoring). Some of the advanced control functions such as rotor speed exclusion zone, active drive train damper, tower top vibration damper, rotor-effective wind speed estimator and curtailment feature [12] are also implemented in the main controller. The individual pitch controller, flap controller, generator servo, blade pitch servos, flap servos and mechanical brake are implemented in different DLLs. Implementation in DLLs can enhance the flexibility and expandability. This modularized implementation approach enables future cooperated developments and verification works within the wind turbine community. The source code will be publicly available at the repository on GitLab website: `https://gitlab.windenergy.dtu.dk/OpenLAC/BasicDTUController`.

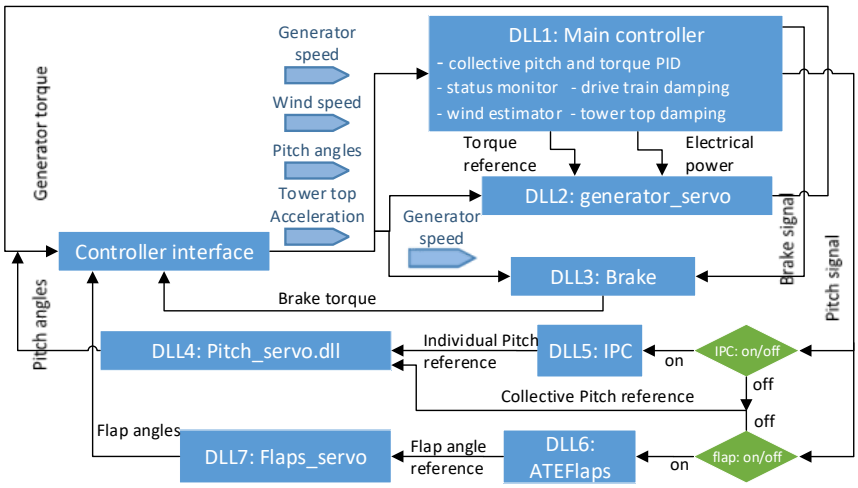

Figure 2: A schematic of the functionalities of the DTU Wind Energy controller

3. Advance control algorithms

Besides the basic turbine control functions such as generator torque and pitch controllers, this section describes some advance control algorithms in DTUWEC.

3.1. Switching between operational regions

In some studies (e.g. [8]), switching is handled by a linear relation between the generator torque and rotor speed. In DTUWEC, a dedicated switching logic is implemented. The switching logic between partial and full load operation is defined as

$$Q_{ref,k} = \max(Q_{min,k}, \min(Q_{max,k}, Q_{PID,k})) \tag{1a}$$

$$Q_{min,k} = (1 - \sigma_h(\bar{\theta}_k))Q^{partial}_{min,k} + \sigma_h(\bar{\theta}_k)Q^{full}_{ref,k} \tag{1b}$$

$$Q_{max,k} = (1 - \sigma_h(\bar{\theta}_k))Q^{partial}_{max,k} + \sigma_h(\bar{\theta}_k)Q^{full}_{ref,k} \tag{1c}$$

where, $Q_{PID,k}$ is the generator torque calculated by the PID torque controller at time step k; $Q^{partial}_{min,k}$ and $Q^{partial}_{max,k}$ are generator torque limits in partial load region; $Q^{full}_{ref,k}$ is the generator torque reference in the full load region at time step k. The equations that describe $Q^{partial}_{min,k}$, $Q^{partial}_{max,k}$ and $Q^{full}_{ref,k}$ can be found in [1]. $\sigma_h(\bar{\theta}_k)$ is the interpolation factor at time step k computed

by the mean pitch angle, $\bar{\theta}_k$, using a linear function defined as follows

$$\sigma_h(\bar{\theta}_k) = \begin{cases} 0 & \bar{\theta}_k \leq \theta_{min,k} \\ \frac{\bar{\theta}_k - \theta_{min,k}}{\theta_{max,k} - \theta_{min,k}} & \theta_{min,k} < \bar{\theta}_k < \theta_{max,k} \\ 1 & \theta_{max,k} \leq \bar{\theta}_k \end{cases} \tag{2}$$

where, $\theta_{max,k} = \theta_{min,k} + \theta_f$, and θ_f is an user-defined angle. When the mean pitch angle is larger than $\theta_{max,k}$, the interpolation factor, $\sigma_h(\bar{\theta}_k)$, remains one until the mean pitch angle becomes lower than the minimum pitch angle, $\theta_{min,k}$. This feature achieves a smooth switching between partial and full load operation and avoids unnecessary switch when the turbine is operating around the rated wind speed region.

3.2. Rotor speed exclusion logic

The rotor speed exclusion logic, as described in the left plot of Figure 3, has 4 states. The state 0 and 3 represent variable speed regions. The generator torque reference,Q_g is calculated by $K\Omega^2$ when the current rotor speed, Ω is either below the lower exclusion zone limit Ω_L or above the upper exclusion zone limit Ω_H. The state 1 and 2 are constant rotor speed regimes (see Fig. 3 left), in which the rotor speed is regulated at either Ω_L or Ω_H by the torque PID controller. The maximum and minimum generator torque limits in the exclusion zone are set to be $Q_{g,max} = 1.05Q_{g,\Omega_L}$ and $Q_{g,min} = 0.95Q_{g,\Omega_H}$ as they are shown in the right plot of Figure 3 and also can be seen in Figure 8. The values of Q_{g,Ω_L} and Q_{g,Ω_H} are provided by the user. During the transients from the state 1 to state 2 and the other way around, the rotor speed set-point is set to be either Ω_H or Ω_L, and the torque PID controller regulates the rotor speed to pass the 3P excitation speed quickly.

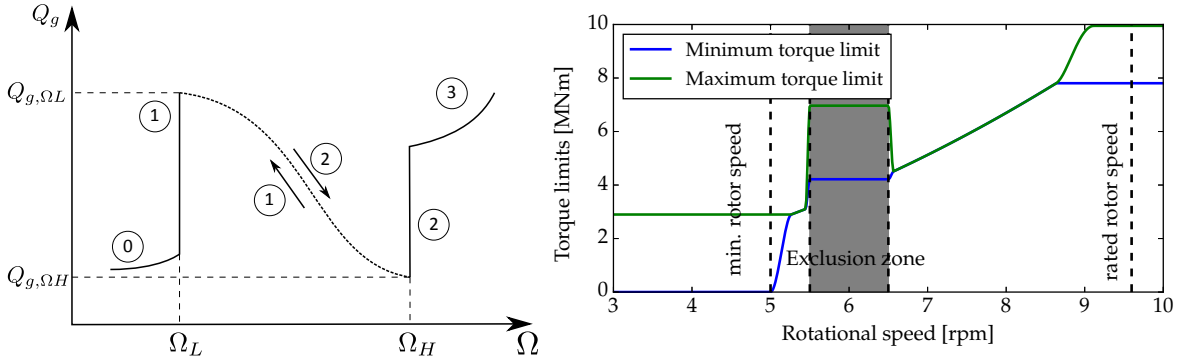

Figure 3: Rotor speed exclusion logic diagram (left); Generator torque limits when the rotor speed exclusion logic is active (right) [1]

3.3. Individual pitch controller

The standard individual pitch control (IPC) inspired by the earlier work of Bossanyi [13] is implemented on top of the collective pitch controller as it was described in [3]. The IPC utilizes three flapwise blade root bending moments and blade azimuth positions to control the pitch angles individually based on Coleman transformations and two PI control loops including the lead compensation to correct the phase lag between these two PI loops. A schematic diagram with the controller details is shown in Figure 4.

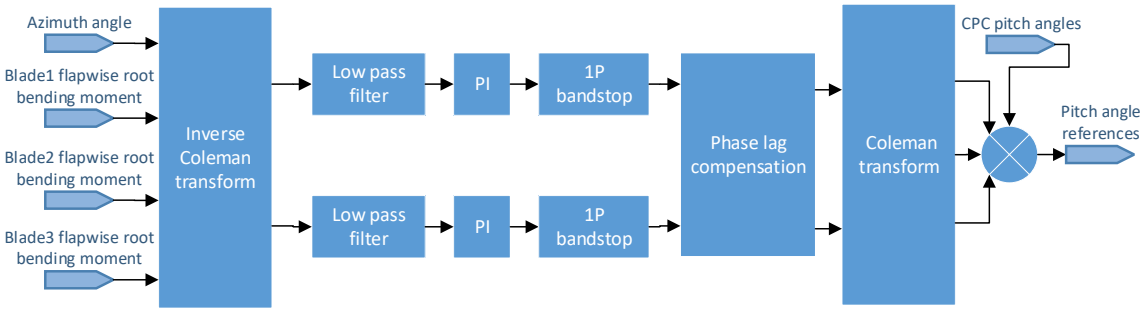

Figure 4: A schematic of the individual pitch controller

3.4. Integrated flap controller

Although a traditional individual flap control is also available in the DTU Wind Energy Controller that is similar to the individual pitch controller, the integrated flap controller needs to be highlighted. It is a result of various projects at DTU in cooperation with the industry [5, 6]. In these projects, certain active flap functionalities have been implemented, providing realistic flap actions which could be utilized in a real wind turbine application. The controller includes three different features shown in Figure 5 and listed as follows:

- **AEP**: Operating-point flap setting (for optimizing AEP and loads ratio);
- **Fatigue**: PID controller (for alleviating fatigue loads);
- **Ultimate**: On-off controller (for alleviating extreme loads).

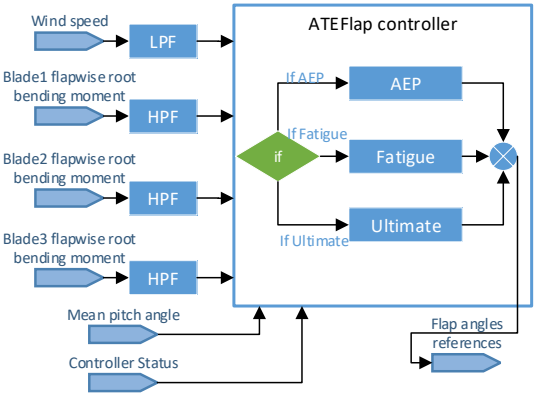

Figure 5: A schematic of the integrated flaps controller

The three features can be utilized independently or together, providing a detailed capability of handling power output, extreme deflection, fatigue and extreme structural loads of the blades.

3.5. Rotor effective wind speed estimation

Rotor effective wind speed is defined as the spatially-averaged wind speeds over the rotor [14]. The rotor effective wind speed estimator in the DTUWEC was developed based on some of the earlier works [15, 16]. The instantaneous rotor effective wind speed is estimated using standard measurements of the turbine rotor speed, pitch angle and generator torque. First, an unknown input observer with a proportional-integral controller is employed to infer the aerodynamic

torque based on a simple first-order drive-train model and generator torque, defined as follows

$$\dot{\hat{\Omega}}(t) = \tfrac{1}{J}(\hat{Q}_\mathrm{a} - Q_\mathrm{g}) + L(\Omega - \hat{\Omega}), \tag{3a}$$

$$\hat{Q}_\mathrm{a} = f_\mathrm{PI}(\Omega - \hat{\Omega}), \tag{3b}$$

where Ω, J denote the rotor speed and inertia, while $Q_\mathrm{a}, Q_\mathrm{g}$ are the aerodynamic and generator torque. The hat notation $\hat{(.)}$ denotes the estimate of the variable, L and f_PI are the observer gain and PI controller, respectively. Subsequently, using the static relationship between the aerodynamic torque, tip-speed ratio λ and pitch angle β, the estimated wind speed $\hat{v}$ can be calculated via a gradient descent method, defined as follows

$$\hat{Q}_\mathrm{a} = \tfrac{1}{2}\rho\pi R^2 \hat{v}^3 C_p(\lambda, \beta)\Omega^{-1}, \tag{4}$$

where ρ denotes the air density and C_p is the power coefficient. The rotor effective wind speed is useful for a number of applications, for example, feed-forward turbine control [16], gain-scheduling controller [17], health monitoring [18] and computation of the power reserve in curtailments [19].

3.6. Minimum thrust coefficient curtailment strategies

One of the curtailment strategies implemented in DTUWEC is the minimum thrust coefficient C_t control strategy developed in a research project, PowerKey [12]. The strategy minimizes the thrust coefficient of a turbine for a given power set-point. This control strategy, although reducing the power output of the de-rated turbines, can improve the aggregate wind farm power output due to the attenuated wake effects. An additional benefit of minimum C_t control is a reduction of fatigue loads farm-wide due to a reduction of the wake deficit and added wake turbulence mentioned in [20, 21]. The concept of minimum C_t control strategy is described as the optimisation problem (5). For a given down regulation percentage ΔP the following minimization problem is then solved to find the solution of tip-speed-ratio λ and pitch angle β. The power coefficient C_p and thrust coefficient C_t of the DTU 10MW reference turbine [22] are illustrated in contour plots as functions of λ and β in Figure 6.

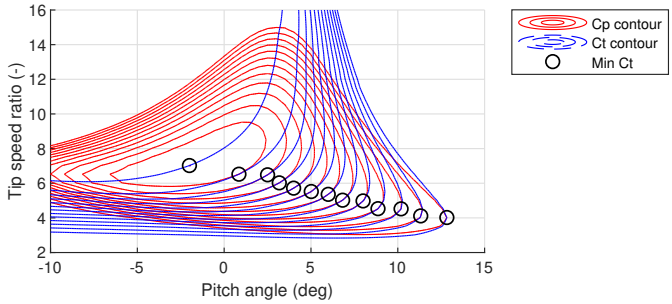

Figure 6: C_p, C_t contours and minimum C_t operational points [12]

The calculated values of λ_d and β_d that satisfy minimum C_t requirement are plotted in Figure 6 and marked as black circles. The power coefficient, $C_{p,d}$, associated with down regulation percentage is tabulated as a function of λ_d and β_d and will be used when calculating the generator torque constant K using Equation 6.

$$\lambda_d, \beta_d = \arg\min_{\lambda,\beta} C_t(\lambda, \beta) \quad \text{Subject to:} \begin{cases} C_{p,d}(\lambda_d, \beta_d) = \Delta P C_{p,max} \\ \lambda_{min} \leq \lambda_d \leq \lambda_{max} \\ \beta_{min} \leq \beta_d \leq \beta_{max} \end{cases} \tag{5}$$

The implementation of this control strategy in the variable-speed region is re-calculating the generator constant, K, tracking the minimum C_t instead of the traditional way that tracks the optimal power coefficient $C_{p,max}$ using the equation defined as

$$K = \frac{1}{2}\rho\pi R^5 \frac{1}{N}\left(\frac{1}{\lambda_d}\right)^3 C_{p,d}(\lambda_d, \beta_d) \tag{6}$$

where, N is the gearbox ratio, R is the rotor radius, ρ is air density and $C_{p,d}$ is the power coefficient value associated with down regulation percentage. In the constant-speed variable-pitch region, the generator speed and torque set-points are determined by the de-rated rotor speed $\Omega_{r,d}$ and the de-rated generator power. The implementation of the switch between partial load and full load region follows the same method as described in the section 3.1.

4. Results

This section presents the simulation results, showing the implemented features of the DTUWEC coupled with the aero-elastic simulation code HAWC2. The DTU 10MW reference wind turbine [22] is used in different simulation scenarios.

4.1. Rotor speed exclusion logic

For demonstrating the rotor speed exclusion control algorithm, simulation with ramp up and ramp down wind speed is performed. The wind speed ramp starts from 4 m/s at 200 s, and increases to 13 m/s at 500 s. Afterwards, the wind speed ramps down to 4 m/s at 800 s. The rotor speed driven by this range of wind speed covers both the first tower fore-aft excitation region and the switching zone between partial and full load. Figure 7 shows the functionality of rotor speed exclusion control, where the time series of rotor speed (left) and the Fast Fourier Transform (FFT) of tower top fore-aft acceleration (right) are displayed for activating and deactivating the exclusion zone. The left plot in Figure 7 shows when the rotor speed is approaching to the resonance speed (5.1 rpm, black dash line), the generator torque PID controller regulates the rotor speed at Ω_L by increasing the generator torque limit to the value of $Q_{g,max}$. When the wind speed is further increased, the generator torque limit is dropped to the value of $Q_{g,min}$, which accelerates the rotor to Ω_H for passing the resonance zone quickly. The right plot in Figure 7 shows that the amplitude of the tower top fore-aft acceleration is suppressed at the resonance frequency (0.255 Hz). Figure 8 shows the generator torque limits and the generator torque reference when the rotor speed exclusion functionality is activated.

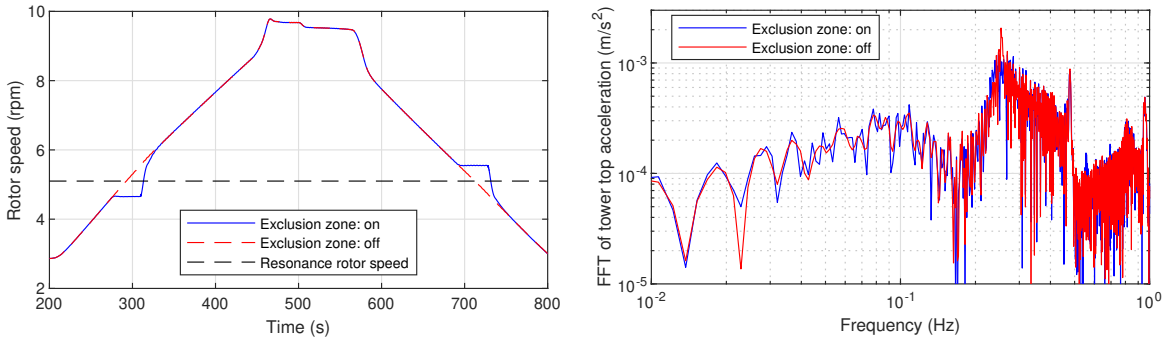

Figure 7: Rotor speed (left) and the FFT of tower top fore-aft acceleration (right)

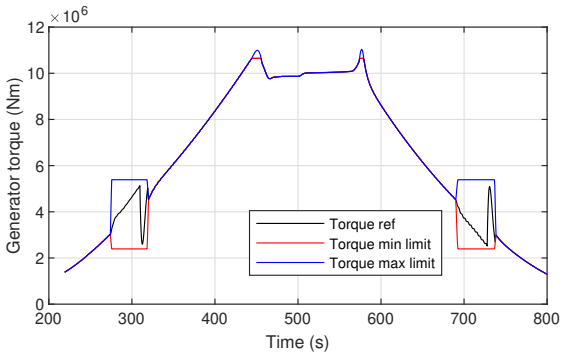

Figure 8: Generator torque maximum limit (blue), generator torque minimum limit (red) and generator torque reference of the PID torque controller (black)

4.2. Normal power production with advanced control features

In this section, the simulation results of the normal power production with turbulent wind cases using the Normal Turbulence Model (NTM) at close to rated and above rated wind speed are presented. The generator torque control strategy is set to constant power control, that indicates in above-rated wind region, the generator torque is inversely proportional to the square of the generator speed. Figure 9 shows the rotor speed, pitch angle, power output and the factor for switching between partial and full loads region at 12 m/s. The turbine starts to operate in the partial load region between 180 seconds and 240 seconds, and the pitch angle goes to zero together with the switch factor. At around 240 seconds, the blades start to pitch, and the switch factor increases to the value of 1 at around 245 seconds, the turbine starts to produce full power.

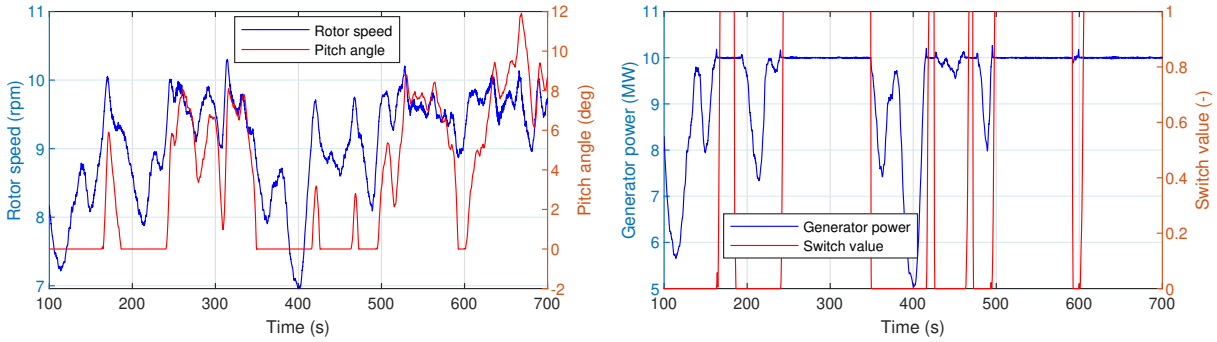

Figure 9: Rotor speed and pitch angle (left), electrical power and switch factor (right) at wind speed of 12 m/s

Figure 10 shows the comparison of the tower bottom fore-aft bending moment and its Fourier transformation at wind speed 12 m/s. When the tower top damper is switched on, the amplitude of the tower bottom bending moment is reduced. This can be seen in the right plot of Fig. 10 where the peak at around 0.25 Hz is reduced when the tower top damper is activated. This demonstrates the correct functionality of the implemented tower top fore-aft damping algorithm.

Simulations are performed at wind speed of 16 m/s with turbulence intensity of 15.4% for testing the individual pitch control feature and flap control feature respectively. The controllers are tuned based on the response of a high-fidelity linear aero-servo-elastic model of the turbine using HAWCStab2 [23]. Figure 11 shows the comparison of the blade pitch rate (left) and the

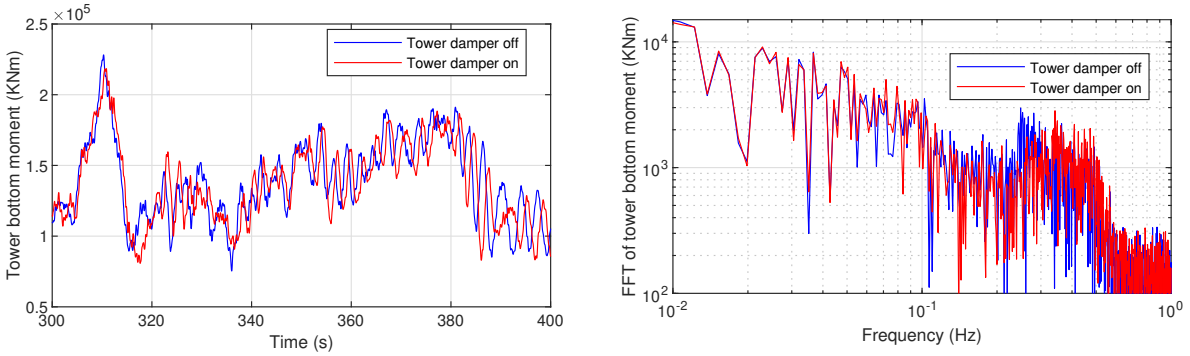

Figure 10: The time series (left) and the FFT (right) of the tower bottom fore-aft bending moment at wind speed of 12 m/s

FFT of blade root flapwise bending moment (right) between collective pitch control, individual pitch control and flap control. As it is shown in the right plot of Fig. 11 the IPC controller results in a larger reduction of the blade flapwise root bending moment than the flap controller at 1P excitation frequency. On the other hand, the blade pitch rate is significantly increased using the individual pitch controller while the flap controller almost does not affect the blade pitch rate of the collective pitch controller.

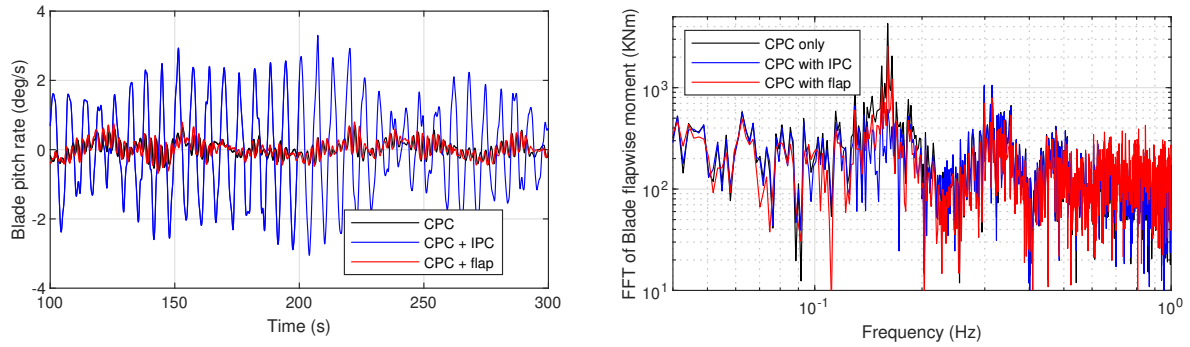

Figure 11: Time series of blade pitch rate (left) and the FFT of the blade flapwise root bending moment (right) at wind speed of 16 m/s

4.3. Curtailment strategy

Figure 12 presents a demonstration of the curtailment control at 90% of the rated power based on the minimum C_t de-rating strategy. The result shows, in the partial load region, the rotor speed follows the minimum C_t operational points determined by the 90% of the rated power and keeps the de-rated rotor speed and the de-rated power output in the full loads region. It also proves that the de-rating strategy performs well when the wind speed steps down.

4.4. Rotor-effective Wind speed estimation

Figure 13 shows the rotor-effective wind speed estimations under turbulent wind cases at both below rated and above rated wind speed region. The blue line is the spatially-averaged wind speed collected from 9 points across the rotor-plane. The results demonstrate the functionality and the performance of wind speed estimation at various operation points. Notice that the current implementation is based on a C_p table that is derived from a rigid turbine, which might cause inaccuracy in the results.

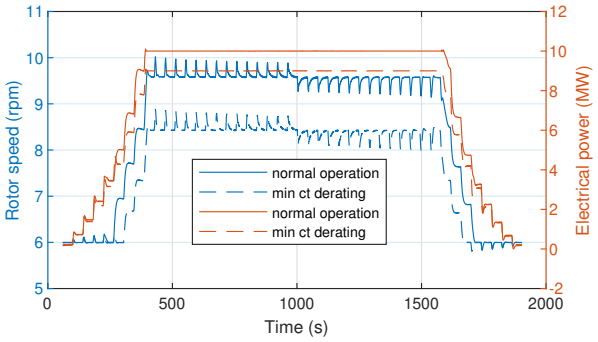

Figure 12: Step response: rotor speed (blue) and electrical power (red) under normal operation (solid line) and curtailment operation (dash line)

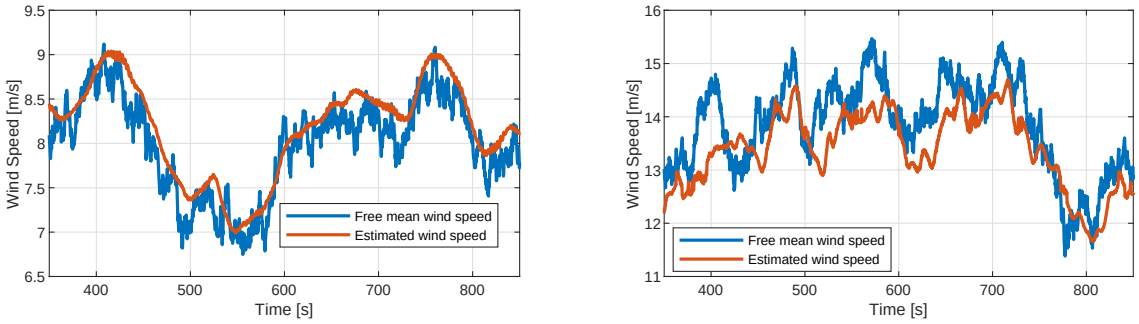

Figure 13: Comparison of the free mean wind speed and its estimate at 8 m/s (left) and 14 m/s (right)

5. Conclusions and future works

In this work, the DTUWEC has been described and demonstrated. The simulation results showed that both the standard functions and the advanced features were working correctly. The DTUWEC is applicable to most commonly used wind turbine aero-elastic codes (e.g. HAWC2, OpenFAST and DNV-GL BLADED), and it is publicly available. The modular setup enables the convenient exchange of the control algorithms for the purpose of testing new algorithms. It provides a wind turbine controller development framework to the scientists and engineers for convenient code-to-code comparison, model evaluation and development of new control algorithms. The future work is to investigate and implement new features, such as closed-loop wind farm control using dynamic induction and wake steering.

Acknowledgement

This research was supported by the PowerKey project (EUDP No. 12558) and TotalControl (EU Horizon 2020 No. 72768). The authors would like to acknowledge Hartvig Hansen, Carlo Tibaldi and Lars Christian Henriksen, who were former employees at DTU Wind Energy and contributed to the development of the Basic DTU Wind Energy Controller.

References

[1] M. H. Hansen and L. C. Henriksen, "Basic DTU wind energy controller," Tech. Rep. DTU Wind Energy No.0028, 2013.
[2] T. J. Larsen and A. M. Hansen, "How to hawc2: the users manual," Tech. Rep. DTU r-1597(en), 2007.
[3] A. Barlas, L. Bergami, M. Hansen, M. Pedersen, D. Verelst, K. Thomsen, and H. Aagaard Madsen, "Load alleviation potential of active flaps and individual pitch control in a full design load basis," 2015, EWEA Annual Conference and Exhibition 2015.

[4] L. Bergami and M. Hansen, "High-fidelity linear time-invariant model of a smart rotor with adaptive trailing edge flaps," *Wind Energy*, vol. 20, no. 3, p. 431–447, 2017.
[5] V. Pettas, A. Barlas, D. Gertz, and H. A. Madsen, "Power performance optimization and loads alleviation with active flaps using individual flap control," *Journal of Physics: Conference Series*, vol. 749, no. 1, p. 012010, 2016.
[6] T. Barlas, V. Pettas, D. Gertz, and H. A. Madsen, "Extreme load alleviation using industrial implementation of active trailing edge flaps in a full design load basis," *Journal of Physics: Conference Series*, vol. 753, p. 042001, sep 2016.
[7] "International Standard IEC 61400-1: Wind turbines - part 1: Design requirements," 2005.
[8] J. Jonkman, S. Butterfield, W. Musial, and G. Scott, "Definition of a 5 MW reference wind turbine for offshore system development," National Rewable Energy Laboratory, Golden, CO 80401, Tech. Rep. NREL/TP-500-38060, 2009.
[9] S. Mulders and J. van Wingerden, "Delft research controller: an open-source and community-driven wind turbine baseline controller," *Journal of Physics: Conference Series*, vol. 1037, p. 032009, jun 2018.
[10] NREL, "Openfast," accessed May 7, 2018. [Online]. Available: https://github.com/OpenFAST/openfast
[11] A. W. H. Lio and F. Meng, "Effective wind speed estimation for wind turbines in down-regulation," *Journal of Physics: Conference Series*, Oct 2019.
[12] F. Meng, A. W. H. Lio, and J. Liew, "The effect of minimum thrust coefficient control strategy on power output and loads of a wind farm," *Journal of Physics: Conference Series*, Oct 2019.
[13] E. A. Bossanyi, "Individual blade pitch control for load reduction," *Wind Energy*, vol. 6, no. 2, pp. 119–128, 2003.
[14] T. Knudsen, T. Bak, and M. Soltani, "Prediction models for wind speed at turbine locations in a wind farm," *Wind Energy*, vol. 14, pp. 877–894, 2011.
[15] K. Z. Østergaard, P. Brath, and J. Stoustrup, "Estimation of effective wind speed," *Journal of Physics: Conference Series*, vol. 75, no. 1, p. 012082, jul 2007.
[16] F. Meng, J. Wenske, and A. Gambier, "Wind turbine loads reduction using feedforward feedback collective pitch control based on the estimated effective wind speed," *Proceedings of the American Control Conference*, vol. 2016-July, pp. 2289–2294, 2016.
[17] D. J. Leith and W. E. Leithead, "Appropriate realization of gain-scheduled controllers with application to wind turbine regulation," *International Journal of Control*, vol. 65, no. 2, pp. 223–248, sep 1996.
[18] F. Meng, T. Meyer, P. Thomas, and J. Wenske, "Observer design and optimization for model-based condition monitoring of the wind turbine rotor blades using genetic algorithm," *Journal of Physics: Conference Series*, vol. 1037, no. 3, 2018.
[19] W. H. Lio, M. Mirzaei, and G. C. Larsen, "On wind turbine down-regulation control strategies and rotor speed set-point," in *Journal of Physics: Conference Series 1037, 032040*, Milan, Italy, 2018.
[20] D. Juangarcia, I. Eguinoa, and T. Knudsen, "Derating a single wind farm turbine for reducing its wake and fatigue," in *Journal of Physics: Conference Series 1037, 032038*, Milan, Italy, 2018.
[21] H. A. Madsen, G. C. Larsen, N. Troldborg, and R. Mikkelsen, "Calibration and validation of the dynamic wake meandering model for implementation in an aeroelastic code," *Journal of Solar Energy Engineering*, vol. 132, no. 041014, pp. 1–14, 2010.
[22] C. Bak, F. Zahle, R. Bitsche, T. Kim, A. Yde, L. C. Henriksen, A. Natarajan, and M. Hansen, "Definition of the dtu 10mw reference wind turbine," Tech. Rep. DTU Wind Energy Report-I-0092, 2013.
[23] M. H. Hansen, "Aeroelastic properties of backward swept blades," in *49th AIAA Aerospace Sciences Meeting including the New Horizons Forum and Aerospace Exposition*. Orlando, FL, USA: American Institute of Aeronautics and Astronautics, Jan. 2011.